


Article

Rationality Research on Pumping Station Location Based on MIKE Model: A Case Study of the Wanfu River Re-Navigation Project

Song Han ¹, Xinyan Yu ¹, Wei Zhang ¹, Guoqing Sang ¹, Yuyu Liu ^{1,*}  and Shiguo Xu ²

¹ School of Water Conservancy and Environment, University of Jinan, Jinan 250022, China; 17860611511@163.com (S.H.); 021871404232@ujn.edu.cn (X.Y.); 15689696598@163.com (W.Z.); stu_sangqq@ujn.edu.cn (G.S.)

² School of Hydraulic Engineering, Dalian University of Technology, Dalian 116024, China; sgxu@dlut.edu.cn

* Correspondence: stu_liuyy@ujn.edu.cn

Abstract: The site selection of hydraulic structures is crucial to the successful implementation of water conservancy projects. Reasonable or not, site selection has a direct impact on the functioning of hydraulic structures, engineering safety, and environmental impact. In this paper, the proposed Wanfu River Guanqiao Ship Lock and Pumping Station engineering is utilised as the object. The MIKE model is executed to simulate both the impact of Guanqiao Ship Lock operation on the water quality of the pumping station intake as well as the effects of pumping station operation on the navigable water level in order to analyse and demonstrate the reasonableness of the pumping station's location. According to the water quality monitoring data of the last three years, the entropy weight method coupled with the comprehensive pollution index method was used to evaluate the water quality of the Wanfu River. A one-dimensional hydrodynamic water quality model was constructed by applying MIKE11, which reveals the change rule of water quality and also demonstrates the safety of navigable water levels. The MIKE21 two-dimensional water quality model, which intuitively displays the spatial and temporal patterns of change of each indicator, was constructed. The results show the following: (1) The evaluation results of the entropy weight method coupled with the comprehensive pollution index method indicate that the water quality of the Wanfu River is Class III, which meets the water intake standard. (2) Concentrations of the indicators are higher in the abundant water period than in the dry water period, in which the water quality is Class IV in June and July. (3) There is no impact of the pump station operating on navigable water levels.

Keywords: MIKE model; water quality assessment; hydrodynamic model; water quality simulation



Citation: Han, S.; Yu, X.; Zhang, W.; Sang, G.; Liu, Y.; Xu, S. Rationality Research on Pumping Station Location Based on MIKE Model: A Case Study of the Wanfu River Re-Navigation Project. *Water* **2023**, *15*, 4207. <https://doi.org/10.3390/w15244207>

Academic Editor: Ataur Rahman

Received: 26 October 2023

Revised: 2 December 2023

Accepted: 4 December 2023

Published: 6 December 2023



Copyright: © 2023 by the authors. Licensee MDPI, Basel, Switzerland. This article is an open access article distributed under the terms and conditions of the Creative Commons Attribution (CC BY) license (<https://creativecommons.org/licenses/by/4.0/>).

1. Introduction

With the rapid development of industry, agriculture, and other sectors, the deterioration of the water environment has become a global water problem [1–3]. The theme of the 18th World Water Conference, “Water for All: Harmony between Humans and Nature”, emphasises that the bottom line for development is environmental quality. Rivers and lakes are the main carriers of terrestrial water resources, and their environmental quality is directly related to the development of society [4]. When hydraulic structures are built, several environmental issues, including river cut-off, deteriorated lake water quality, and decreased biodiversity, can occur [5]. Even though hydraulic structures can have certain negative environmental effects, throughout the design and construction stages, several safeguards can be put in place to lessen these impacts. Evaluating environmental impacts using hydrodynamic water quality model simulations is a common practice.

Hydrodynamic modelling is the rule of the changes in the hydraulic elements of water and other liquids (flow, water level and flow velocity, etc.) over time and space, described by a set of mathematical equations and numerically solved under certain initial

and boundary conditions [6,7]. French scientist Saint-Venant proposed the famous Saint-Venant equation, which discusses the shallow water body under the condition of free liquid surface to do asymptotic non-constant flow law of motion, which provides a theoretical basis for the subsequent research of hydrodynamic simulation [8,9]. Hansen succeeded in simplifying Saint-Venant's equations using the periodicity of the tides and proposed a computational model for two-dimensional numerical simulations [10]. As science advances, numerical simulation gradually assumes a significant role. Many academics have begun to simulate and evaluate the forms and processes of evolution in terms of water environment characteristics using numerical modelling techniques on multi-regional river networks. The migration pattern of pollutants in water bodies, the self-purification ability of water bodies, and the changing pattern of water quality can be studied and simulated using water quality models [11,12]. At the beginning of the 20th century, Streeter first proposed a water quality model (S-P) of oxygen balance, which laid a solid foundation for the development of water quality models in later years [13]. Common examples of hydrological numerical simulation software include the MIKE software (1978) model developed by the Danish Hydraulic Institute (DHI), the HEC-RAS program developed by the US Army Corps of Engineers' Engineering Hydrology Center (HEC), the MODFLOW model developed by the US Geological Survey, and the WASP and EFDC models proposed by the US Environmental Protection Agency (EPA), as well as Delft3D, CE-QUAL-R1, CE-QUAL-W2, etc. Each of these models has its specific application conditions; for example, the MODFLOW model was developed by the USGS in the 1980s as a suite of software dedicated to the numerical simulation of groundwater flow in pore media. The MIKE software is powerful in hydrodynamic and water quality modelling and can be used to accurately process and analyse complex problems [14–17]. In the Water Quality module, the MIKE software allows the user to create different pollutant composition templates based on the pollutants in a specific study area, thus more accurately modelling and predicting changes in the water quality of a water body. Using the MIKE software (2007), Tang et al. [18] established a one-dimensional hydrodynamic model to calculate the hydraulic characteristics of the river channel of the South-to-North Water Diversion Middle Line Project, and based on it, a one-dimensional advective diffusion model of TP, NH₃-N, COD_{mn}, and F was built to simulate the sudden pollution accidents with emergency response measures. Based on the measured data, Zhu et al. [19] investigated the hydrodynamic and water quality changes in the Erhai Lake by applying the MIKE software to build a two-dimensional coupled hydrodynamic and water quality model, which screened the capacity of the water environment and the abatement of pollutant discharges, to provide guidance for the management and effective use of water resources in the Erhai Lake. A one-dimensional water quantity and quality model was established by Wang et al. [20] with the MIKE software, and a comparative study of two water allocation schemes was conducted by selecting water cycle and water quality as evaluation indicators. On the basis of the theory of the two-dimensional mathematical modelling of the water environment, Zhang et al. [21] constructed a water environment model of the Baiguishan Reservoir using the MIKE21 model, which analysed the evolutionary characteristics and improvement of the water environment of the reservoir under the conditions of six ecological recharge scenarios. With meteorological and hydrological data and water quality data, Li et al. [22] used the MIKE model to simulate the water quality evolution pattern of Donghu Lake. Using the HD and Ecolab modules of MIKE, Jia et al. [23] simulated the hydrodynamic and water quality conditions in the Bohai Bay, China, together with predicting the impacts of shoreline changes. Mali et al. [24] conducted 2D numerical simulations using the MIKE21 model to determine the origin and fate of pollutants in the port basin. The results showed that the contaminants mainly come from the outside port, with a tendency to accumulate in the inner basin. As can be seen, the MIKE software is extensively used for hydrodynamic analysis and water quality modelling, pollutant migration in water bodies, and water quality enhancement.

The Guanqiao Lock and Pumping Station is a re-navigation project on the Wanfu River, and it is of great significance for socio-economic development. This study, which

examined the proposed Guanqiao Ship Lock and Pumping Station while taking both ample and dry water periods into account, aimed to (1) evaluate whether the water quality of Wanfu River met the water abstraction standards using the entropy weight method coupled with the integrated pollution index method, (2) simulate the impact of the ship lock on water quality at the pumping station intake under rule operation using the MIKE model, and (3) model whether pumping station abstractions had an impact on navigable water levels. By constructing a coupled hydrodynamic water quality model, the spatial and temporal distribution law of water body flow and water quality status are revealed, so as to scientifically plan and manage water resources and achieve a win–win situation for both the economy and environment.

2. Materials and Methods

2.1. Study Area

Wanfu River is located in the southwestern part of Shandong Province, east of Nansihu, north of Zhuzhao New River, south of the East Fish River, and west of the North Branch of the East Fish River. It originates in Chulou, Chengwu County, Heze and flows eastward to Liuzhuang Village, Mamiao Township, Jinxiang County, then enters Jining City; the Jining section of the river crosses 11 towns and villages in the four counties (districts) of Jinxiang, Yutai, Weishan, and Rengcheng, and is injected into the Nanyang Lake in Dazhou Village of Rengcheng District. It is the backbone of a favourable river in southwestern Shandong Province for waterlogging, flood control, alkalinity modification, and irrigation, and it belongs to the Huaihe River Basin and the system of the Nansihu Lake. The length of the Xinwanfu River system is 77.3 km (41.5 km in Jining City), with a watershed area of 1283 km² (370 km² in Jining City), and the main tributaries are the Liulin River, the Anji River, the Jincheng River, the Peng River, the Dasha River, and the Xiaowu River. Located in the east-central part of Heze City and the southern part of Jining City, Shandong Province, the Xinwanfu River Channel consists of the northern branch of the Dongyu River and the Xinwanfu River, collectively known as the Xinwanfu River Channel. The lowest navigable water level of the channel from Guanqiao Ship Lock to Guanqiao Pumping Station is 32.80 m.

Guanqiao Pumping Station is the source project of Kirin Lake Reservoir and the proposed Wanfeng Reservoir in Juye County, and its main function is to take water from Wanfu River Lane into the Reservoir and to take care of agricultural irrigation on both sides of the river under the premise of meeting the domestic and industrial water use in Juye County. The water quality requirements for its water intake are high, and it needs to meet the requirements of Class III water. Guanqiao Pumping Station is located on the left bank of Wanfu River channel, 1.4 km downstream of the confluence of Fengshou River, south of Guanqiao Village. The pumping station hub project consists of a diversion canal, inlet sluice gate, culvert through the embankment, front pool, inlet pool, pump house, outlet pipe, and management area.

Guanqiao Ship Lock is located 900 m upstream of Guanqiao Pumping Station, at the location of S242 Liaoshang Highway bridge. The upper and lower lock heads of the Guanqiao Ship Lock are of a monolithic structure consisting of reinforced concrete solid slabs and box-type side piers, with plane dimensions of 28.0 m × 40.0 m in length × width, and a bottom slab thickness of 2.8 m. The total length of the lock chamber is 234 m, of which the effective length is 230 m, the sedation section is 4m, and the width of the chamber is 23 m. The geographical location of the proposed hydraulic structures is shown in Figure 1, and a schematic of the navigation channel is displayed in Figure 2.

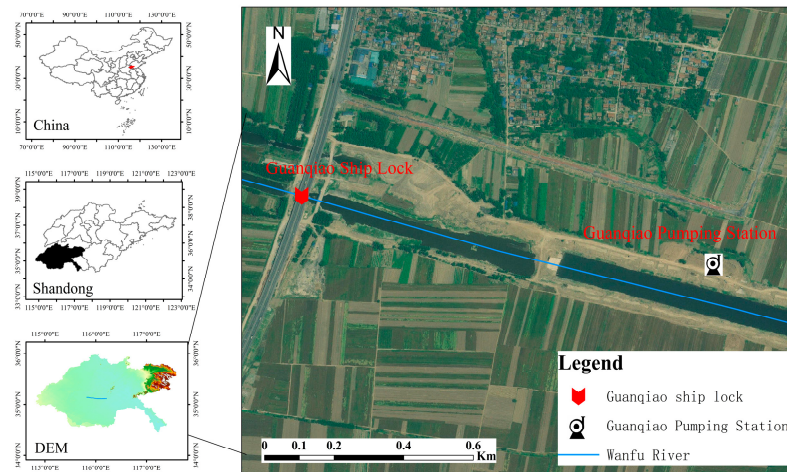


Figure 1. Geographic location of proposed hydraulic structures.

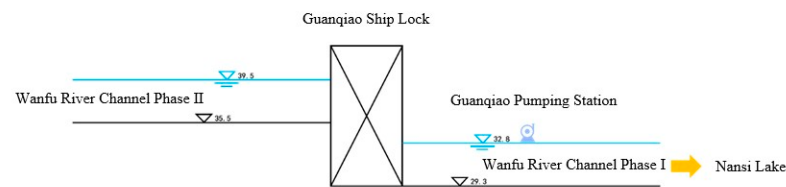


Figure 2. Channel Schematic.

2.2. Entropy Weighted Coupled Comprehensive Pollution Index Method

The comprehensive pollution index method is based on the single-factor pollution index method and uses arithmetic averaging for statistics, which can visually identify the difference between water quality and the functional requirements of the water body [25]. The formula is:

$$P = \frac{1}{n} \sum_{j=1}^n \frac{c_j}{c_0} \tag{1}$$

here, n is the type of pollutant; P is the integrated pollution index; c_j is the measured value of the j -th pollutant; c_0 is the evaluation standard value of the j -th pollutant.

Traditional integrated pollution index method uses equal weight assignment method for calculation, which does not take into account the variability among different water quality indicators. Entropy weight method is an assignment method to determine the weights of indicators according to the variability of the original data [26], in which the entropy value of each indicator reflects the degree of disorder of information. Normally, the smaller the entropy weight is, the less disordered the system is and the closer the information representing the indicator is. Hence, establishing the weights through the entropy weighting method can try to exclude the interference of human factors in the calculation of the weights of the indicators so as to make the evaluation results more scientific and credible.

Firstly, the raw data were standardised. Assume that the original evaluation matrix is formed by m evaluation objects and n evaluation indicators $A = (A_{ij})_{m \times n}$, where A_{ij} is the measured value of the i -th object for the j -th pollutant ($i = 1, 2, \dots, m$; $j = 1, 2, \dots, n$). Normalising matrix A yields matrix $B = (b_{ij})_{m \times n}$, where $b_{ij} = C_{ij} / \sum_{i=1}^m C_{ij}$;

$$C_{ij} = \begin{cases} A_{ij} / \max_{1 \leq i \leq m} A_{ij} (\text{Positive}) \\ \min_{1 \leq i \leq m} A_{ij} / A_{ij} (\text{Negative}) \end{cases}$$

The entropy e_j of the j -th water quality indicator is:

$$e_j = -\frac{1}{\ln m} \sum_{i=1}^m b_{ij} \ln b_{ij} \quad (2)$$

For the j -th water quality indicator, the weight ω_j is:

$$\omega_j = \frac{1 - e_j}{\sum_{j=1}^n (1 - e_j)} \quad (3)$$

Based on the entropy weighting method, the comprehensive pollution index is:

$$P' = \sum_{j=1}^n \omega_j P_j \quad (4)$$

here, P' is the comprehensive pollution index based on entropy weights.

2.3. Model Equation

2.3.1. MIKE11

(1) MIKE11 Hydrodynamic Module

The MIKE11 hydrodynamic module (HD) is based on vertically integrated equations for the conservation of matter and momentum, i.e., a set of equations for one-dimensional non-constant-flow Saint Venant's equations to simulate the flow state of a river [27,28]. The Abbott–Ionescu 6-point implicit difference format was used for the solution, i.e., the water level and flow were not calculated simultaneously at each calculation point, and a sequential approach was taken to calculate the water level and flow in alternating order as follows:

$$\frac{\partial Q}{\partial x} + \frac{\partial A}{\partial t} = q \quad (5)$$

$$\frac{\partial Q}{\partial t} + \frac{\partial \left(\alpha \frac{Q^2}{A} \right)}{\partial x} + gA \frac{\partial h}{\partial x} + \frac{gQ|Q|}{c^2 A R} = 0 \quad (6)$$

here, x and t are the spatial and temporal coordinates of the calculation point, A is the area of the flow section, Q is the overflow, h is the water level, q is the lateral inflow, C is the Xie Cai coefficient, R is the hydraulic radius, α is the momentum modification coefficient, and g is the gravitational acceleration.

(2) MIKE11 Water Quality Module

Using the MIKE11 water quality model, which automatically extracts the hydrodynamic conditions generated by the HD module and incorporates convective diffusive and biochemical transport processes into the water ecology simulation, the model is used to describe the interactions of the different substances in the aquatic ecosystem and their respective morphological changes [29]. The basic equation is the one-dimensional convection–diffusion equation:

$$\frac{\partial A_1 C_1}{\partial t} + \frac{\partial Q C_1}{\partial x} - \frac{\partial}{\partial x} \left(AD \frac{\partial C_1}{\partial x} \right) = C_2 q - AKC_1 \quad (7)$$

here, A_1 is the cross-sectional area, m^2 ; C_1 is the mass concentration of the pollutant, mg/L ; D is the longitudinal diffusion coefficient, m^2/s ; C_2 is the source and sink item, mg/L ; K is the linear attenuation coefficient, $1/d$.

2.3.2. MIKE21

(1) MIKE21 Hydrodynamic Module

For the MIKE 21 2D hydrodynamic model, the principal governing equations are the continuity equation for planar 2D flow, the momentum equation for planar 2D flow, and the hydrostatic pressure assumption [30], as follows:

$$\frac{\partial h}{\partial t} + \frac{\partial h\bar{u}}{\partial x} + \frac{\partial h\bar{v}}{\partial y} = hS \quad (8)$$

$$\begin{aligned} \frac{\partial h\bar{u}}{\partial t} + \frac{\partial h\bar{u}^2}{\partial x} + \frac{\partial h\bar{u}\bar{v}}{\partial y} = f\bar{v}h - gh\frac{\partial\eta}{\partial x} - \frac{h}{\rho_0}\frac{\partial P_\alpha}{\partial x} - \frac{gh^2}{2\rho_0}\frac{\partial P}{\partial x} + \\ \frac{\tau_{ax}}{\rho_0} - \frac{\tau_{hx}}{\rho_0} - \frac{1}{\rho}\left(\frac{\partial S_{xx}}{\partial x} + \frac{\partial S_{xy}}{\partial x}\right) + \frac{\partial(hT_{xx})}{\partial x} + \frac{\partial(hT_{xy})}{\partial x} + hu_sS \end{aligned} \quad (9)$$

$$\begin{aligned} \frac{\partial h\bar{v}}{\partial t} + \frac{\partial h\bar{v}^2}{\partial y} + \frac{\partial h\bar{u}\bar{v}}{\partial x} = f\bar{u}h - gh\frac{\partial\eta}{\partial y} - \frac{h}{\rho_0}\frac{\partial P_\alpha}{\partial y} - \frac{gh^2}{2\rho_0}\frac{\partial P}{\partial y} + \\ \frac{\tau_{ay}}{\rho_0} - \frac{\tau_{hy}}{\rho_0} - \frac{1}{\rho}\left(\frac{\partial S_{yx}}{\partial y} + \frac{\partial S_{yy}}{\partial x}\right) + \frac{\partial(hT_{yx})}{\partial x} + \frac{\partial(hT_{yy})}{\partial y} + hv_sS \end{aligned} \quad (10)$$

here, h is the static water depth; t is time; x , y , and z constitute the right-handed Cartesian coordinate system; u and v are the components of the flow velocity in the x , y direction; \bar{u} and \bar{v} constitute the flow velocity averaged along the water depth; S is the source and sink item; f is the Coriolis parameter; g is the acceleration of gravity; η is the height of the water surface relative to the undisturbed base, i.e., the water level; ρ_0 is the density of the reference water; P_α is the local barometric pressure; and ρ is the water density. τ_{ax} , τ_{ay} , τ_{hx} , and τ_{hy} are the components of the water flow shear stress in the x , y direction at the water surface and riverbed boundary; S_{xx} , S_{xy} , S_{yx} , and S_{yy} are the radial stress components; T_{xx} , T_{xy} , T_{yx} , and T_{yy} are the horizontal viscous stresses; and u_s and v_s constitute the velocity of water flow in the source and sink term.

(2) MIKE21 Water Quality Module

The water quality water ecology module (ECO Lab) of the MIKE21 model can be used to describe changes in bacterial content, organic matter degradation, and oxygen environment in the water body based on the principle of using a coupled set of differential equations for biochemical reactions to reflect the factors that increase or decrease each water quality parameter variable over time, and whose state variables satisfy non-conservation equations [31]; see formula below:

$$\frac{\partial c}{\partial t} + u\frac{\partial c}{\partial x} + v\frac{\partial c}{\partial y} + w\frac{\partial c}{\partial z} = D_x\frac{\partial^2 c}{\partial z^2} + D_y\frac{\partial^2 c}{\partial z^2} + D_z\frac{\partial^2 c}{\partial z^2} + S_c + P_c \quad (11)$$

here, c is the concentration of the state variable; u , v , and w represent the flow rate; D_x , D_y , and D_z are the diffusion coefficients; S_c is the source and sink term, $u\frac{\partial c}{\partial x} + v\frac{\partial c}{\partial y} + w\frac{\partial c}{\partial z}$ is a convective term; $D_x\frac{\partial^2 c}{\partial z^2} + D_y\frac{\partial^2 c}{\partial z^2} + D_z\frac{\partial^2 c}{\partial z^2}$ is a diffusion term; P_c represents the various chemical reaction processes in the water column that affect changes in substance concentrations.

2.4. Modelling Building

2.4.1. MIKE 11

In accordance with the principle of river generalisation, the river was generalised according to its location and specific conditions, such as topography and terrain, and it was determined that the beginning point of the calculation of this model was the Nanwangzhuang river section and the endpoint was the Xiangzimiao river section. Parameters are entered and running rules are set up in the control structure module of the river network file to simulate the working of locks and pumping stations. At the same time, according to the channel section design drawings, we obtained the section starting point distance and riverbed elevation data, which generated the corresponding section file. According to the channel section design drawings, we determined the section start distance and riverbed

elevation data, edited it into a text file by format, and imported it into MIKE to generate the section file.

Boundary conditions included external and internal boundary conditions. The so-called external boundaries were those endpoints of river segments in the model that were not connected to other river segments. The internal boundary was where the flow into or out of the modelled reach occurred from a point or section of the internal reach of the model. In this simulation, only the boundary conditions at the two ends of the river section were set up, with the upper boundary being the Nanwangzhuang section and the lower boundary being the Xiangzimiao section. Hydrodynamic modelling was based on daily flow and water level data, with flow-time data being used for the upper boundary and water level-time data for the lower boundary. Boundary conditions for the water quality model were set to monthly water quality monitoring data in 2022, with simulated water quality indicators of BOD₅, NH₃-N, TP, and COD.

In order to enhance the simulation accuracy of the model, the riverbed roughness, i.e., Manning's coefficient, was set for the hydraulic characteristics of different sections of the Wanfu River, with the parameter values shown in Table 1. Parameters of the AD module include attenuation coefficients for BOD₅, NH₃-N, TP, and COD; settling rates; resuspension rates; critical rates for settling; and more. The diffusion coefficient of the model was taken as 2 m²/s, while the values of the comprehensive attenuation coefficients of each pollutant are shown in Table 2.

Table 1. Manning's coefficients for analogue segments.

Reach	Nanwangzhuang–Guanqiao Lock	Guanqiao Lock–Xiangzimiao
Manning's coefficient	0.02	0.03

Table 2. Combined attenuation factor for each pollutant.

Reach	Comprehensive Attenuation Coefficient/d ⁻¹			
	BOD ₅	NH ₃ -N	TP	COD
Nanwangzhuang–Guanqiao Lock	0.080	0.070	0.060	0.067
Guanqiao Lock–Xiangzimiao	0.077	0.067	0.010	0.062

2.4.2. MIKE 21

The boundary of the simulation area and the projection coordinates of the terrain data were adopted as WGS_1984_UTM_Zone_50N. Import boundary and terrain data into the Mesh Generator to generate a terrain file. Based on the morphology of the Manifold River channel and the needs of the study, a triangular grid with better stability was used and some narrow sections were refined. After smoothing, a relatively good grid was obtained, and it had 9636 computational grids and 5136 computational nodes (Figure 3).

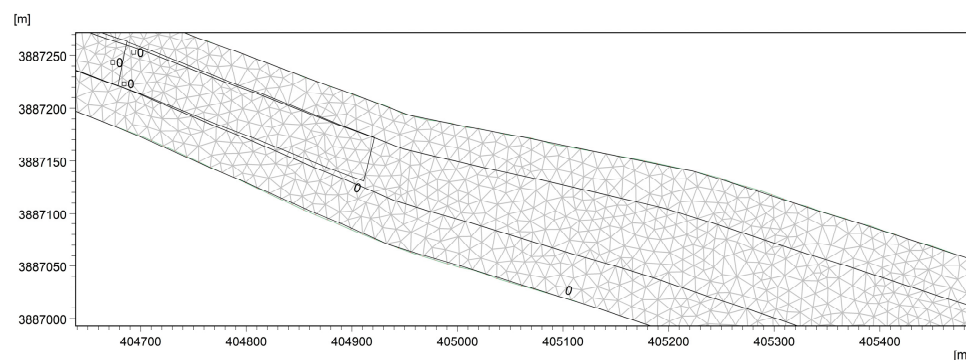


Figure 3. Grid file.

Data on river flows, water levels, and water quality were obtained from jurisdictional water departments. The multi-year average hydrological data of Nanwangzhuang and Xiangzimiao were adopted as the hydrodynamic boundary; the initial concentrations of BOD₅, NH₃-N, TP, and COD were set with reference to the monitoring data of state-controlled cross sections and provincial-controlled cross sections. In addition to the topography of the river network, initial and boundary conditions, parameters such as dry and wet water depths and riverbed roughness, needed to be set. Parameters of the model were set as follows: the dry water depth $h_{\text{dry}} = 0.005$ m, the inundation depth $h_{\text{flood}} = 0.05$ m, and the wet water depth $h_{\text{wet}} = 0.1$ m. The eddy viscosity coefficient was set to 0.28, the Manning's coefficient value was set to $32 \text{ m}^{1/3}/\text{s}$, and the diffusion coefficient was $2 \text{ m}^2/\text{s}$. Specific parameters are shown in Table 3.

Table 3. Values of parameters.

Parameter	Value
Dry depth	0.005 m
Flooding depth	0.05 m
Wet depth	0.1 m
Eddy viscosity coefficient	0.28
Transverse diffusion coefficient	$2 \text{ m}^2/\text{s}$
Manning's coefficient	$32 \text{ m}^{1/3}/\text{s}$

3. Results and Discussion

3.1. Water Quality Assessment of Wanfu River

(1) Calculation of entropy weights

We calculated the entropy weights of each water quality indicator based on the water quality data of monitoring sections in 2020–2022 in Nanwangzhuang and Xiangzimiao (Formula (3)). The entropy weighting method considers the differences in the degree of variability of the water quality indicators and determines the weights according to the magnitude of variability. The weights of the indicators are shown in Table 4.

Table 4. Weighting of water quality indicators near Guanqiao, 2020–2022.

Year	DO	COD _{Mn}	NH ₃ -N	TP	BOD ₅
2020	0.06	0.05	0.60	0.17	0.12
2021	0.07	0.05	0.58	0.20	0.10
2022	0.07	0.04	0.64	0.15	0.10

(2) Evaluation criteria of comprehensive pollution index based on entropy weight method

According to the environmental quality standard for surface water (GB3838-2002), the threshold value of Class III water is adopted as the baseline value. By multiplying the ratio of the standard limit value of each index to the standard limit value of Class III water bodies by the weight of the corresponding index, the improved evaluation standard of comprehensive pollution index based on the entropy weighting method can be obtained, as shown in Table 5.

Table 5. Evaluation Criteria of Comprehensive Pollution Index Improved Based on Entropy Weight Method.

Evaluation Level	I	II	III	IV	V
value	0.27	0.54	1	1.51	2.09

(3) Evaluation results of the comprehensive pollution index method based on entropy weights

Table 6 displays the evaluation outcomes for the comprehensive pollution index technique based on entropy weight. The assessment results show that the monitoring section near the proposed Guanqiao Pumping Station meets the water quality standard of Class III for surface water, which means it is of good quality and meets the requirements for water intake. Because the pumping station needs to meet the domestic and industrial water intake, as well as agricultural irrigation on both sides of the river, its water intake quality must meet the requirements of Class III water. The evaluation results of the integrated pollution index method based on entropy weight improvement showed that the water quality near the pumping station intake meets the Class III water standard. As can be seen from the composite pollution index, the general trend in water quality for 2020–2022 shows that it is getting better each year.

Table 6. Evaluation results of the comprehensive pollution index method based on entropy weights.

Section	2020	2021	2022	Evaluation Criteria
Nanwangzhang	0.76	0.67	0.60	III
Xiangzimiao	0.56	0.69	0.59	III

3.2. MIKE11 Results and Analysis

3.2.1. Water Level

Influenced by the upstream water inflow and downstream water return, the simulation area basically meets the navigable water level demand, and the simulation results are presented in Figure 4. During the dry season, the upstream of the locks may not be able to meet the navigational demand due to insufficient water inflow, which is because the Phase II project has not yet been implemented, and the data have been derived from the pre-construction period, which may deviate from the final result. However, the downstream of the locks is influenced by the return of water from the Nansihu Lake, basically meeting the demand for navigational water level.

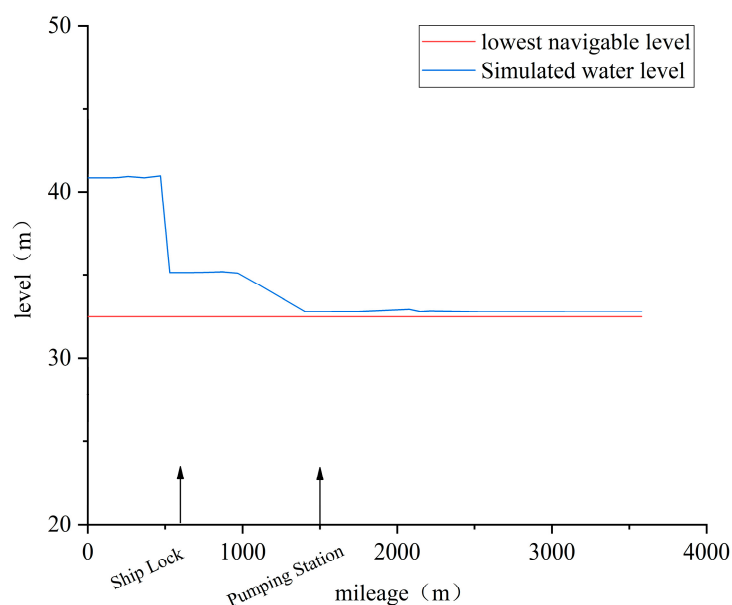


Figure 4. Water level changes in the modelled area.

3.2.2. Characteristics of Spatial and Temporal Variations in Water Quality

Changes in the maximum values of water quality indicators along the upstream to downstream course are shown in Figure 5. Spatially, upstream to downstream water quality

shows a trend of getting better. The maximum concentration of BOD₅ along the course is 6.4 mg/L, which is classified as water IV. NH₃-N maximum concentration is 0.83 mg/L, which is classified as Class II water. With a maximum concentration of 0.389 mg/L, TP is classified as Class IV water. COD maximum concentration is 40.5 mg/L, which is classified as Class V water. Lock operation has had a significant impact on water quality in the section of the river between the lock and the pumping station, with essentially no influence on water quality further afield. This is because the opening and closing of the locks during operation exchanges upstream and downstream waters. The temporal variation of each indicator at the pump station location is shown in Figure 6. Temporally, the concentrations of the indicators were much greater in the abundant water period than in the dry water period, especially for COD. This is primarily due to increased rainfall allowing pollutants such as pesticides and fertilisers to enter the river. It is recommended that pumping station withdrawals avoid periods of heavy continuous rainfall.

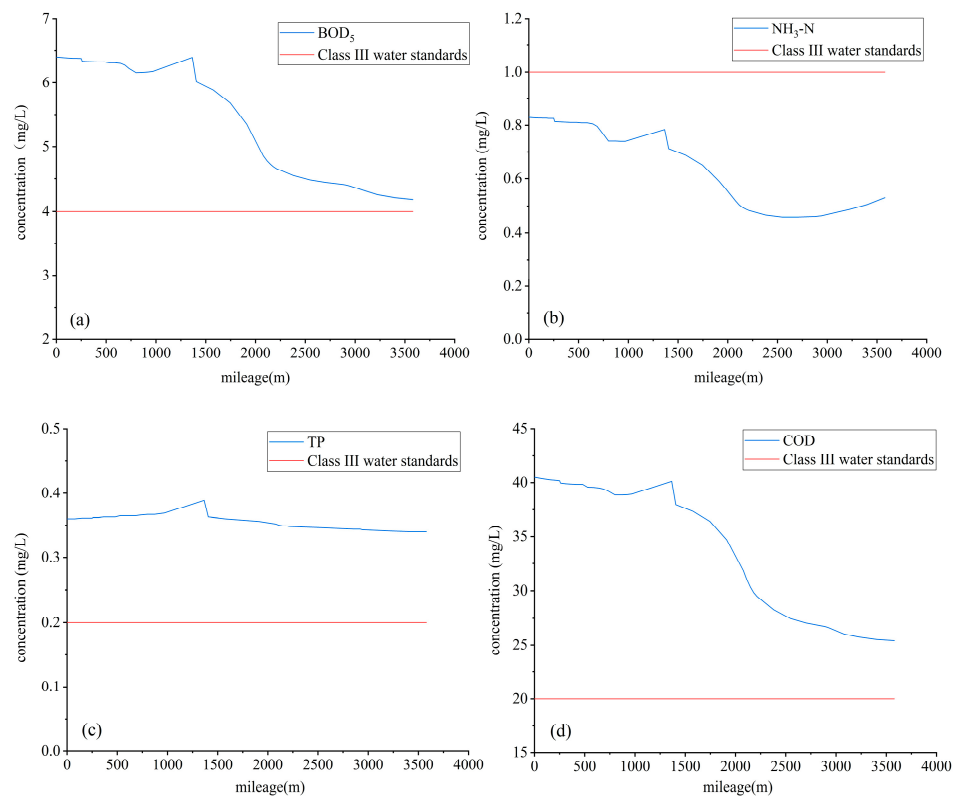


Figure 5. Changes in maximum values of water quality indicators along the route. (a) Concentration of BOD₅; (b) concentration of NH₃-N; (c) concentration of TP; (d) concentration of COD.

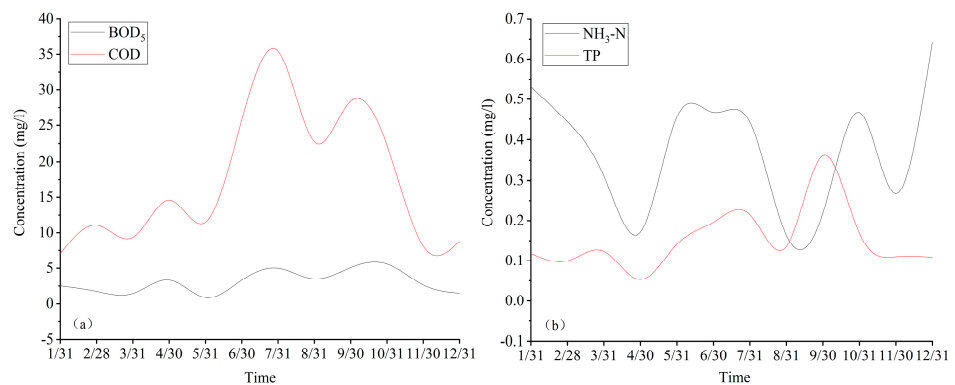


Figure 6. Temporal variation of indicators at pumping station locations. (a) Concentrations of BOD₅ and COD over time; (b) concentrations of NH₃-N and TP over time.

3.3. MIKE21 Water Quality Modeling Results and Analysis

Depending on the available information and data analysis, it has been determined that the Wanfu River has an abundant water period from June to September, and the flow upstream of the lock is cut off in December and January, so the Wanfu River’s dry period is eventually defined as the months from February to May. In accordance with the environmental quality standards for surface water, the standard limits of each indicator are set to different colours, which can visually display the water quality status.

3.3.1. Characteristics of Spatial and Temporal Variations in Indicators during Wet Season

(1) BOD₅

The spatial distribution of BOD₅ concentrations during periods of abundant water is shown in Figure 7. From June to September, the BOD₅ concentration at the pumping station intake increased and then decreased, with the highest BOD₅ concentration occurring in July. In July, the highest BOD₅ concentration was 4.0–4.4 mg/L, belonging to Class IV water; the lowest was 3.2–3.6 mg/L, belonging to Class III water. As the simulation time proceeded, the water quality at the intake of the Guanqiao Pumping Station stabilised at Class III water, meeting the water quality requirements. The cause of the concentration exceeding Class III water in July was that the water level reached the criteria for the opening of the control gates, which opened and released water to regulate the water level, and the upstream water bodies with poorer water quality entered the downstream.

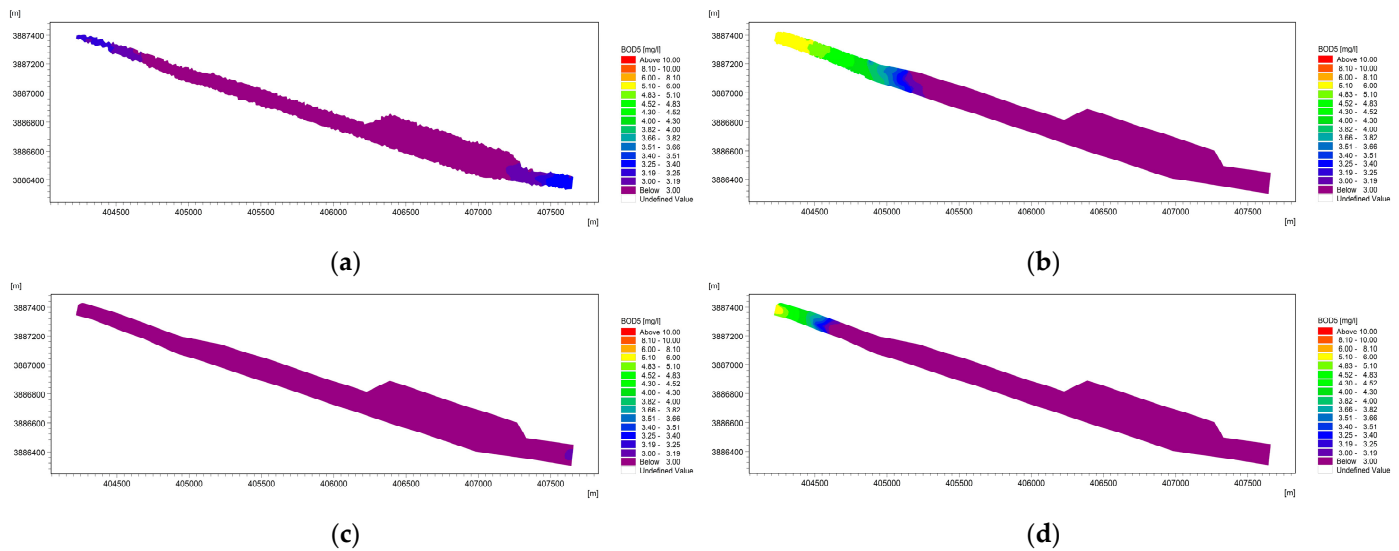


Figure 7. Spatial distribution of BOD₅ concentration during the period of water abundance. (a) BOD₅ distribution in June; (b) BOD₅ distribution in July; (c) BOD₅ distribution in August; (d) BOD₅ distribution in September.

(2) NH₃-N

Figure 8 depicts the regional distribution of NH₃-N concentrations during the period of ample water. During the modelling process, the ammonia nitrogen concentration at the intake of the Guanqiao Pumping Station was 0.400.94 mg/L at its highest, which was classified as Class II water. The ammonia nitrogen content at the Guanqiao Pumping Station intake stabilised at the Class II water standard and satisfied the water quality standards as the simulation progressed.

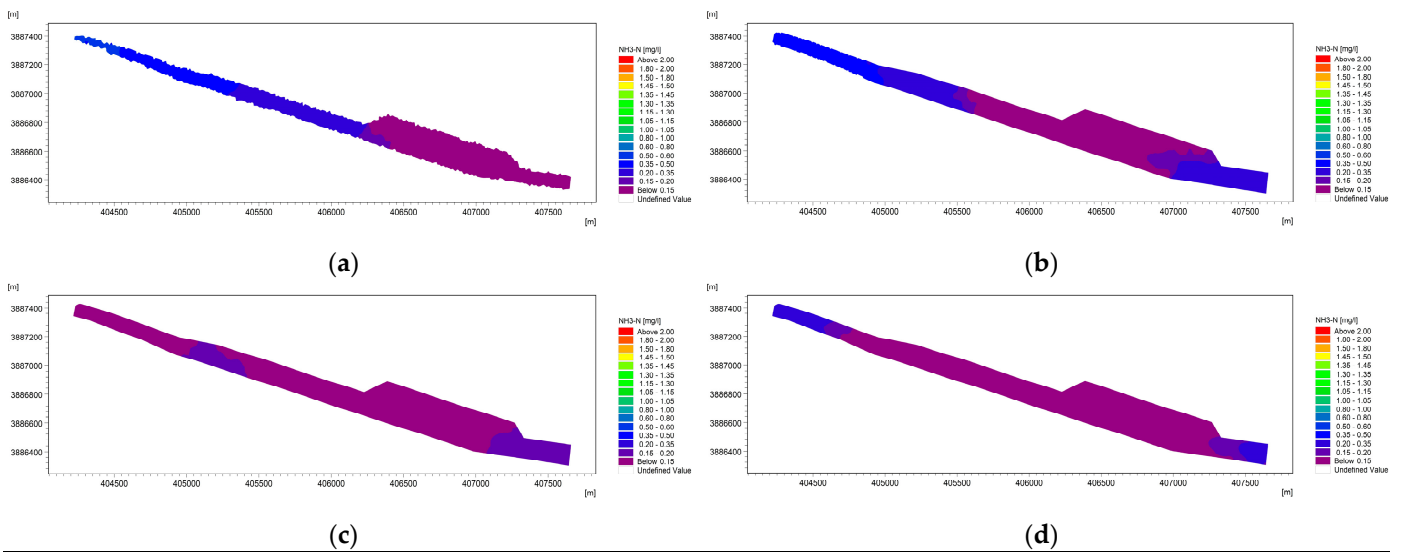


Figure 8. Spatial distribution of $\text{NH}_3\text{-N}$ concentration during the time of abundant water. (a) $\text{NH}_3\text{-N}$ distribution in June; (b) $\text{NH}_3\text{-N}$ distribution in July; (c) $\text{NH}_3\text{-N}$ distribution in August; (d) $\text{NH}_3\text{-N}$ distribution in September.

(3) TP

In Figure 9, the regional distribution of TP concentrations during periods of plenty water is depicted. TP concentrations were highest in September during the simulation. The maximum TP concentration in September was 0.275–0.300 mg/L, when the water quality was Class IV; the minimum concentration was 0.075–0.10 mg/L, when the water quality was Class II. With the simulation, the TP concentration at the intake of the Guanqiao Pumping Station stabilised at Class III water, which meets the water quality standard. Due to the long period of heavy rainfall, a large amount of P was carried into the river, resulting in a high TP concentration in September.

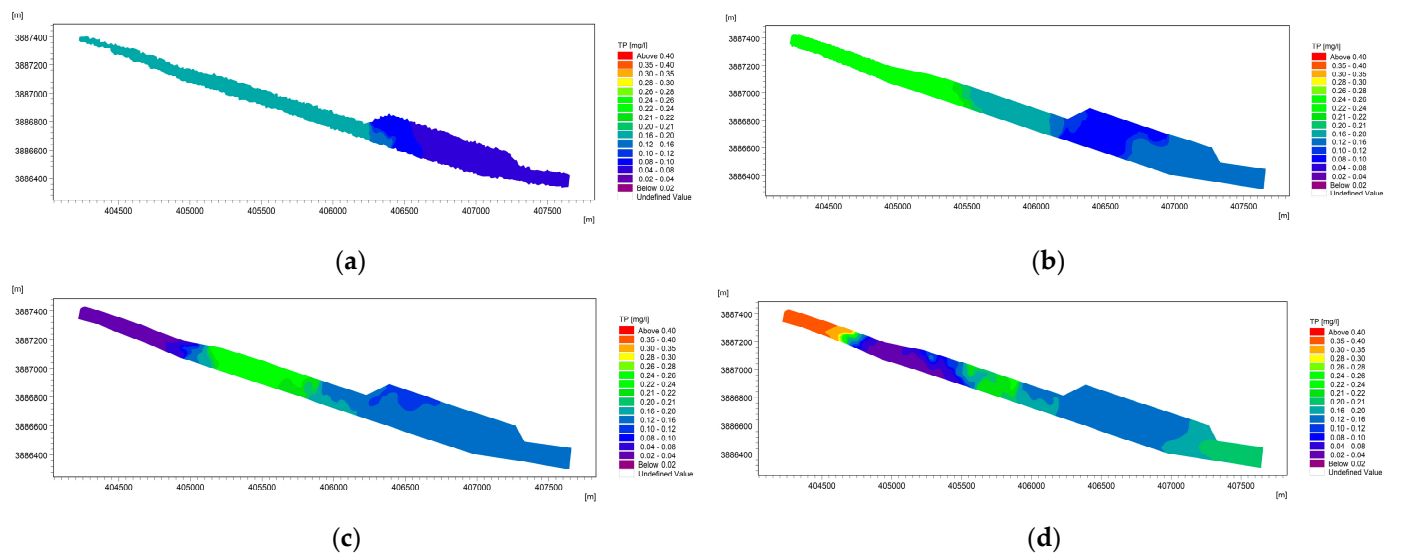


Figure 9. Spatial distribution of TP concentration during the period of water abundance. (a) TP distribution in June; (b) TP distribution in July; (c) TP distribution in August; (d) TP distribution in September.

(4) COD

The temporal spatial distribution of COD concentrations during the period of abundant water is shown in Figure 10. During the simulation period, the COD concentration was highest in July. It was in July that the highest COD concentrations were found, ranging from 30.0 to 32.5 mg/L, and the water quality was classified as Type IV water. According to the information, a heavy rain occurred in July 2020, the concentration of organic matter in the water body increased, and the COD concentration then surged; the lowest COD concentration was 18~20 mg/L, and the water quality belonged to the Class III water category. When the modelling continued, the COD concentration level stabilised at Class III water and the water quality requirements were met.

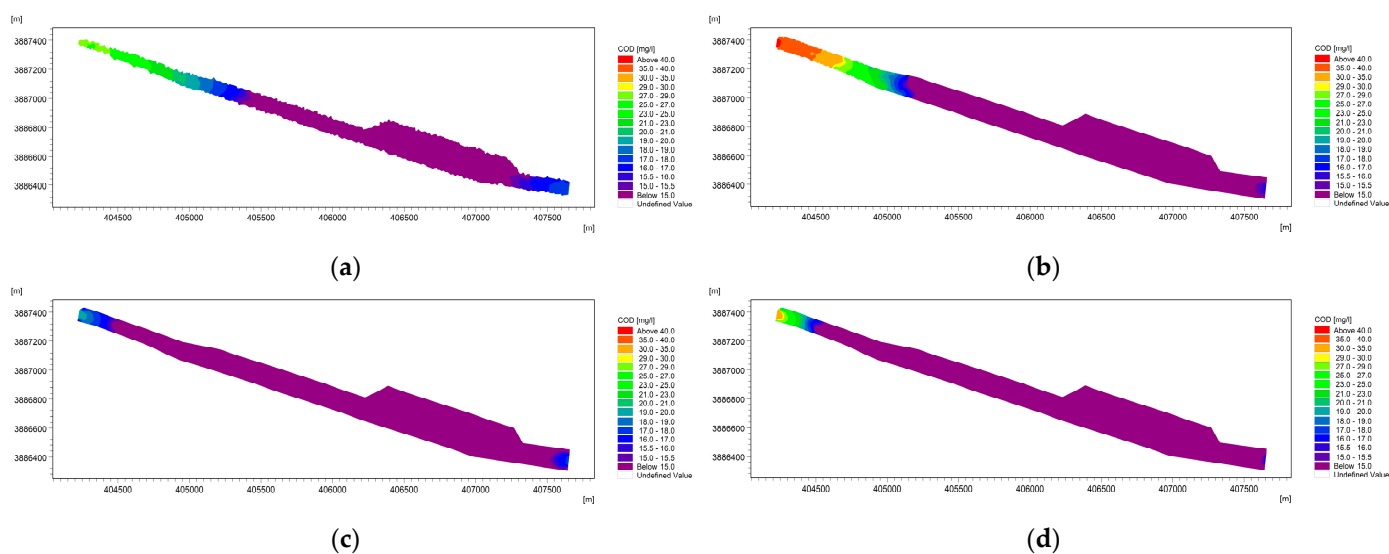


Figure 10. Spatial distribution of COD concentration during the period of water abundance. (a) COD distribution in June; (b) COD distribution in July; (c) COD distribution in August; (d) COD distribution in September.

3.3.2. Characteristics of Spatial and Temporal Variations in Indicators during Dry Period

(1) BOD₅

See Figure 11 for the spatial distribution of BOD₅ concentrations during the dry period. During the simulation period, the BOD₅ concentration was higher and the water quality was poorer in April. In April, the highest BOD₅ concentrations ranged from 2.75 to 3.00 mg/L, which made them classified as Class III water; the lowest values ranged from 2.25 to 2.50 mg/L, which made them classified as Class III water. With the simulation, the water quality at the intake of the Guanqiao Pumping Station stabilised to Class III water, which fulfilled the water quality requirements.

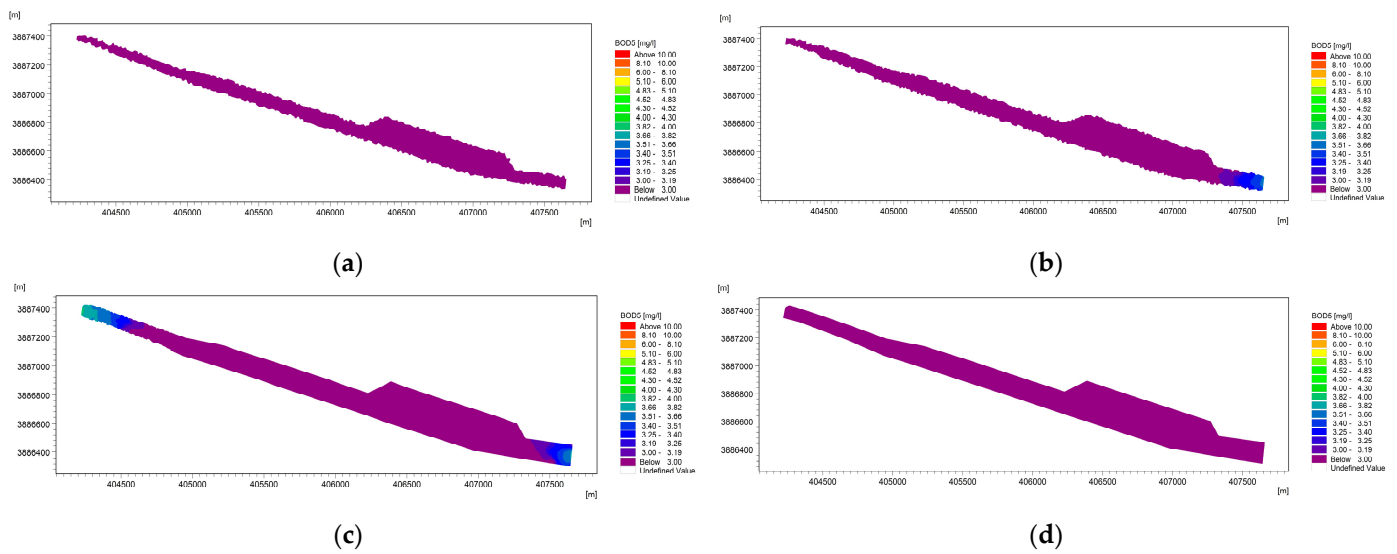


Figure 11. Spatial distribution of BOD₅ concentration during dry water period. (a) BOD₅ distribution in February; (b) BOD₅ distribution in March; (c) BOD₅ distribution in April; (d) BOD₅ distribution in May.

(2) NH₃-N

The spatial distribution of NH₃-N concentration during the dry period is shown in Figure 12. During the analogue procedure, the ammonia nitrogen concentration at the intake of the Guanqiao Pumping Station was 0.460–0.465 mg/L at the highest time, which meant it belonged to the Class II water category. As the simulation went on, the concentration of ammonia nitrogen at the intake of the Guanqiao Pumping Station stabilised at the standard of Class II water, which meets the water quality requirements. It is obvious from the results that the water quality becomes better from upstream to downstream.

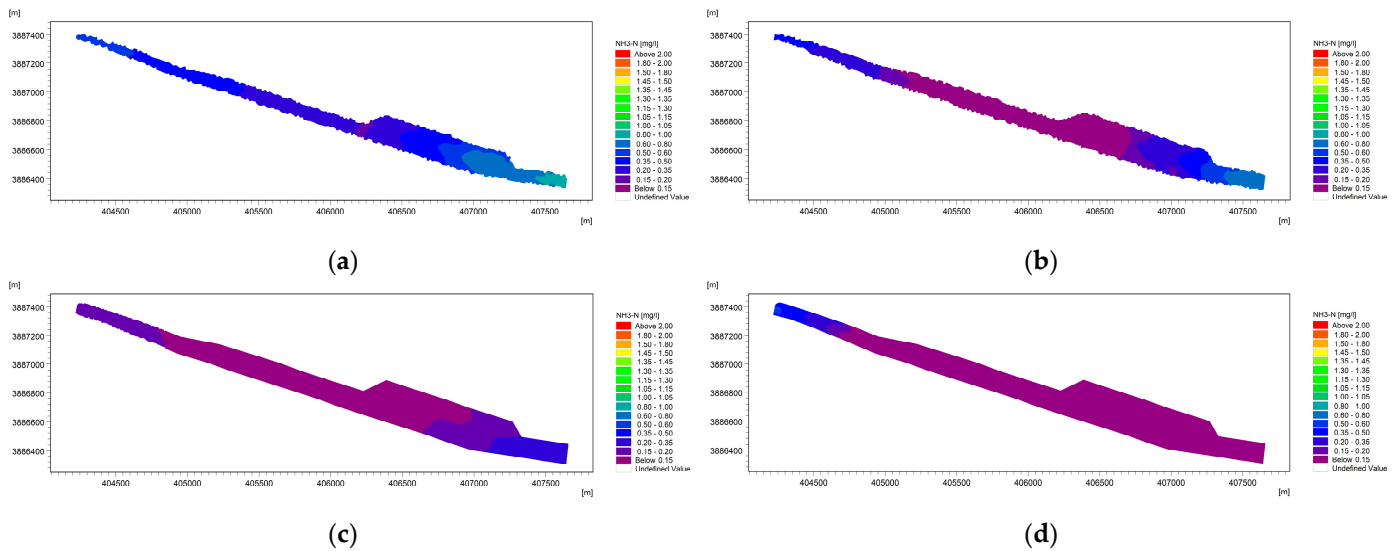


Figure 12. Distribution of NH₃-N concentrations during the dry period. (a) NH₃-N distribution in February; (b) NH₃-N distribution in March; (c) NH₃-N distribution in April; (d) NH₃-N distribution in May.

(3) TP

The spatial distribution of TP concentrations during the dry period is shown in Figure 13. During the simulation period, the highest concentration of TP was recorded in May due to increased rainfall, which increased phosphorus levels in the water column; the

maximum concentration was 0.138 mg/L, and the water quality was classified as Type III. The lowest concentration of TP in May ranged from 0.054 to 0.060 mg/L, and the water quality was classified as Class II water. As the simulations proceeded, the TP concentration at the intake of the Guanqiao Pumping Station stabilised to Class III water, which meets the water quality requirements.

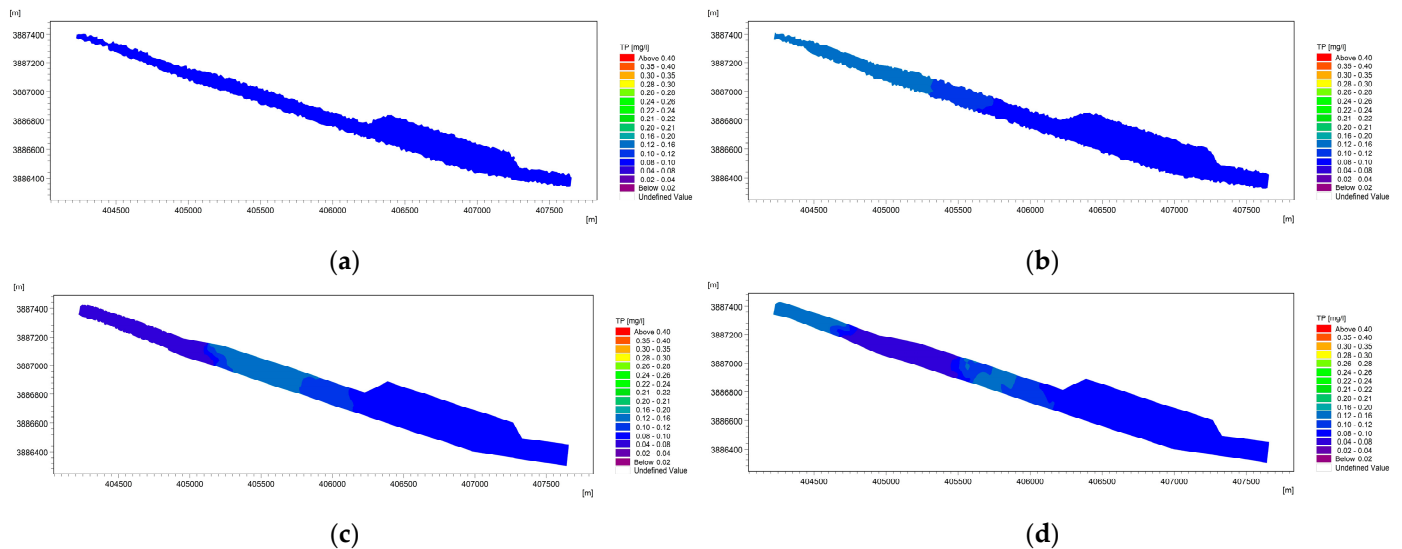


Figure 13. Spatial distribution of TP concentration during dry water period. (a) TP distribution in February; (b) TP distribution in March; (c) TP distribution in April; (d) TP distribution in May.

(4) COD

Figure 14 illustrates the regional distribution of COD concentrations over the dry period. During the simulation period, the COD concentration was highest in April. In April, the maximum COD concentration was 15–16 mg/L, with a water quality of Class III; the minimum was 10–12 mg/L, which indicated Class II water. As the simulation continued, the COD level stabilised at Class II water, satisfying the water quality requirements.

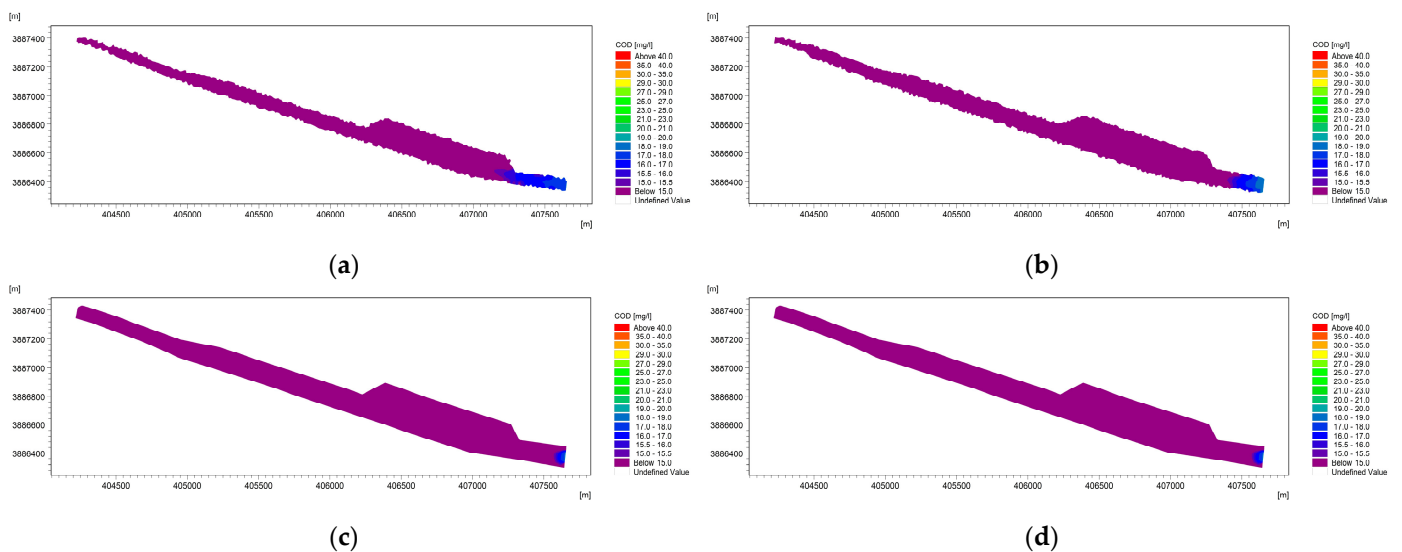


Figure 14. Spatial distribution of COD concentration during dry water period. (a) COD distribution in February; (b) COD distribution in March; (c) COD distribution in April; (d) COD distribution in May.

3.3.3. Water Quality Analyses during Periods of Abundance and Desiccation

Using the results of MIKE21, the maximum concentration of each indicator near the intake in different months was derived, which was evaluated using the entropy-weighted coupled comprehensive pollution index method to evaluate the water quality during the abundant and dry periods. Water quality data and evaluation results are shown in Table 7. As can be seen from the table, the water quality is poorer during the high water period compared to the low water period; the water quality near the pumping station intake is poorer in June and July, and a large number of pollutants are washed into the river by rainfall because of rainfall and agricultural activities. Therefore, if the location is not changed, it is recommended that the pumping station's intake requirements be met through time scheduling. In contrast, the solution of moving the location of the pumping station downwards is more scientifically sound.

Table 7. Water quality data and evaluation results.

Periods	Months	BOD ₅	NH ₃ -N	TP	COD	Pollution Index	Evaluation Criteria
Wet period	February	2.91	0.46	0.10	13.43	0.54	III
	March	2.71	0.43	0.12	14.39	0.54	III
	April	3.00	0.37	0.13	16.01	0.55	III
	May	2.51	0.44	0.13	15.51	0.56	III
	June	4.05	0.94	0.29	20.29	1.08	IV
Dry season	July	4.40	0.88	0.31	17.09	1.07	IV
	August	3.63	0.74	0.23	15.58	0.87	III
	September	3.44	0.60	0.33	15.72	0.91	III

4. Conclusions

Using an integrated pollution index method that is entropy-weight-based, we assessed the water quality in the region around the Guanqiao Pumping Station. Our conclusions demonstrated that the proposed Guanqiao Pumping Station's monitoring section's water quality satisfies the requirements for Class III surface water and is improving yearly. We considered the assignment of weights among the indicators to make the evaluation results more objective, providing a reference for the study of the local water environment.

MIKE11 concentrates on the simulation of river hydrodynamics and the study of river engineering problems, whose structure control module in the river network file is able to simulate, perfectly, the operation of locks and pumping stations. The MIKE11 results indicate that subject to the upstream water inflow and downstream return water, the locks and pumping stations satisfy the navigable water level requirements after completion. Increased rainfall during times of abundance, particularly in June and July, has led to an increase in the quantity of contaminants entering the water body from upstream. While the construction of the ship locks has had a considerable effect on the water quality close to the pumping station, it has had little to no effect farther away from the locks and during dry periods. The MIKE21 Ecolab module provides a wealth of water quality parameters and, secondly, has user-friendly visualisation tools to facilitate the analysis of model results. The BOD₅, TP, and COD concentrations in the modelled area during the ample water phase ranged from Class III to Class IV water, while the NH₃-N concentration was of Class II water, according to the MIKE21 data. During the dry period, the concentrations of BOD₅ and TP were Class III water, whereas those of NH₃-N and COD were Class II water. Based on the maximum concentration of each indicator at the pumping station intake, the entropy weighting method coupled with the integrated pollution index method was used for water quality evaluation, which resulted in similar conclusions to those of MIKE11. Similarly, rainfall is the primary factor contributing to the elevated concentrations of the indicators. If the location of the pumping station remains the same, it is recommended that the water quality needs of the intake be met through timing scheduling. In contrast, it is more scientifically sound to move the location of the pumping station downstream. By

demonstrating the reasonableness of the pumping station location, the waste of resources and possible environmental impacts can be avoided.

Author Contributions: Conceptualization, S.H. and W.Z.; software, G.S.; investigation, S.H.; resources, X.Y., G.S. and Y.L.; data curation, Y.L.; writing—original draft preparation, S.H.; writing—review and editing, Y.L.; visualization, G.S. and S.X.; project administration, X.Y., G.S. and Y.L. All authors have read and agreed to the published version of the manuscript.

Funding: This study was supported by the National Natural Science Foundation of China (No. 42377077), the Social Science Planning Research Project of Shandong Province (NO. 23CGLJ04), and the Open Research Fund of the Henan Key Laboratory of Water Resource Conservation and Intensive Utilization in the Yellow River Basin (NO. HAKF202202).

Data Availability Statement: The data that support the findings of this study are available from the corresponding author (Y.L.) upon reasonable request.

Conflicts of Interest: The authors declare no conflict of interest.

References

- Abdi, B.; Bozorg-Haddad, O.; Loáiciga, H.A. International Water Comprehensive Organization (IWCO): Creating alliances for improved water management and solving water conflicts. *AQUA-Water Infrastruct. Ecosyst. Soc.* **2023**, *72*, 465–478. [[CrossRef](#)]
- Kim, S.; Devineni, N.; Lall, U.; Kim, H.S. Sustainable Development of Water Resources: Spatio-Temporal Analysis of Water Stress in South Korea. *Sustainability* **2018**, *10*, 3795. [[CrossRef](#)]
- Yeleliere, E.; Cobbina, S.J.; Duwiejuah, A.B. Review of Ghana’s water resources: The quality and management with particular focus on freshwater resources. *Appl. Water Sci.* **2018**, *8*, 93. [[CrossRef](#)]
- Boyer, A.-L.; Comby, E.; Flaminio, S.; Le Lay, Y.-F.; Cottet, M. The social dimensions of a river’s environmental quality assessment. *Ambio* **2019**, *48*, 409–422. [[CrossRef](#)] [[PubMed](#)]
- Long, Y.; Yang, Y.; Li, Y.; Zhang, Y. Rapid prediction of pollutants behaviours under complicated gate control for the middle route of South-to-North water transfer project. *Environ. Technol.* **2021**, *42*, 4208–4220. [[CrossRef](#)]
- Yi, Y.; Tang, C.; Yang, Z.; Zhang, S.; Zhang, C. A One-Dimensional Hydrodynamic and Water Quality Model for a Water Transfer Project with Multihydraulic Structures. *Math. Probl. Eng.* **2017**, *2017*, 2656191. [[CrossRef](#)]
- Shan, C.; Guo, H.; Dong, Z.; Liu, L.; Lu, D.; Hu, J.; Feng, Y. Study on the river habitat quality in Luanhe based on the eco-hydrodynamic model. *Ecol. Indic.* **2022**, *142*, 109262. [[CrossRef](#)]
- Vieira, J.H.D. Conditions governing the use of approximations for the Saint-Venant equations for shallow surface water flow. *J. Hydrol.* **1983**, *60*, 43–58. [[CrossRef](#)]
- Greenhill, A.G. The Elastica Researches of Barré de Saint-Venant. *Nature* **1890**, *41*, 458–459. [[CrossRef](#)]
- Hansen, W. Dissected Drift Plain of Southeastern Nebraska. *Econ. Geogr.* **1936**, *12*, 381–391. [[CrossRef](#)]
- Jiang, T.; Zhong, M.; Cao, Y.-J.; Zou, L.-J.; Lin, B.; Zhu, A.-P. Simulation of Water Quality under Different Reservoir Regulation Scenarios in the Tidal River. *Water Resour. Manag.* **2016**, *30*, 3593–3607. [[CrossRef](#)]
- Uddin, M.G.; Nash, S.; Rahman, A.; Olbert, A.I. A comprehensive method for improvement of water quality index (WQI) models for coastal water quality assessment. *Water Res.* **2022**, *219*, 118532. [[CrossRef](#)]
- Streeter, H.W. Natural Stream Purification as Applied to Practical Measures of Stream Pollution Control. *Sew. Work. J.* **1938**, *10*, 747–753.
- Jia, P.; Wang, Q.; Lu, X.; Zhang, B.; Li, C.; Li, S.; Li, S.; Wang, Y. Simulation of the effect of an oil refining project on the water environment using the MIKE 21 model. *Phys. Chem. Earth Parts A/B/C* **2018**, *103*, 91–100. [[CrossRef](#)]
- Peng, K.; Li, J.; Zhou, X.; Li, H.; Xie, W.; Zhang, K.; Ullah, Z. Simulation and control of non-point source pollution based on MIKE model: A case study of Danjiang river basin, China. *Ecohydrol. Hydrobiol.* **2023**, *in press*. [[CrossRef](#)]
- Liu, Q.; Wang, D.; Zhang, Y.; Wang, L. Flood Simulation Analysis of the Biliu River Basin Based on the MIKE Model. *Complexity* **2021**, *2021*, 8827046. [[CrossRef](#)]
- Malcangio, D.; Cuthbertson, A.; Meftah, M.B.; Mossa, M. Computational simulation of round thermal jets in an ambient cross flow using a large-scale hydrodynamic model. *J. Hydraul. Res.* **2020**, *58*, 920–937. [[CrossRef](#)]
- Tang, C.; Yi, Y.; Yang, Z.; Cheng, X. Water pollution risk simulation and prediction in the main canal of the South-to-North Water Transfer Project. *J. Hydrol.* **2014**, *519*, 2111–2120. [[CrossRef](#)]
- Zhu, C.; Liang, Q.; Yan, F.; Hao, W. Reduction of Waste Water in Erhai Lake Based on MIKE21 Hydrodynamic and Water Quality Model. *Sci. World J.* **2013**, *2013*, 958506. [[CrossRef](#)] [[PubMed](#)]
- Wang, Q.; Wang, Y.; Lu, X.; Jia, P.; Zhang, B.; Li, C.; Li, S.; Li, S. Impact assessments of water allocation on water environment of river network: Method and application. *Phys. Chem. Earth Parts A/B/C* **2018**, *103*, 101–106. [[CrossRef](#)]
- Zhang, X.; Duan, B.; He, S.; Lu, Y. Simulation study on the impact of ecological water replenishment on reservoir water environment based on Mike21—Taking Baiguishan reservoir as an example. *Ecol. Indic.* **2022**, *138*, 108802. [[CrossRef](#)]

22. Li, X.; Huang, M.; Wang, R. Numerical Simulation of Donghu Lake Hydrodynamics and Water Quality Based on Remote Sensing and MIKE 21. *ISPRS Int. J. Geo-Inf.* **2020**, *9*, 94. [[CrossRef](#)]
23. Jia, H.; Shen, Y.; Su, M.; Yu, C. Numerical simulation of hydrodynamic and water quality effects of shoreline changes in Bohai Bay. *Front. Earth Sci.* **2018**, *12*, 625–639. [[CrossRef](#)]
24. Mali, M.; Malcangio, D.; Dell' Anna, M.M.; Damiani, L.; Mastroianni, P. Influence of hydrodynamic features in the transport and fate of hazard contaminants within touristic ports. Case study: Torre a Mare (Italy). *Heliyon* **2018**, *4*, e00494. [[CrossRef](#)] [[PubMed](#)]
25. Zhang, G.; Zhang, Q.; Shang, K. Eco-Engineering Technologies and Achievements of Projects for Reconstructing Landscape Water from Aquaculture Ponds in Shanghai. *Water* **2023**, *15*, 2881. [[CrossRef](#)]
26. Bao, Q.; Yuxin, Z.; Yuxiao, W.; Feng, Y. Can Entropy Weight Method Correctly Reflect the Distinction of Water Quality Indices? *Water Resour. Manag.* **2020**, *34*, 3667–3674. [[CrossRef](#)]
27. Fakouri, B.; Mazaheri, M.; Samani, J.M. Management scenarios methodology for salinity control in rivers (case study: Karoon River, Iran). *J. Water Supply: Res. Technol.-Aqua* **2018**, *68*, 74–86. [[CrossRef](#)]
28. Yan, Q.; Jing, Z.; Xia, Z.; Zhang, S. Flood Control Capacity of the Three Gorges Project for Different Frequency Floods. *Environ. Eng. Sci.* **2021**, *38*, 1195–1205. [[CrossRef](#)]
29. Parker, G.T.; Droste, R.L.; Rennie, C.D. Coupling model uncertainty for coupled rainfall/runoff and surface water quality models in river problems. *Ecohydrology* **2013**, *6*, 845–851. [[CrossRef](#)]
30. Wang, Q.; Peng, W.; Dong, F.; Liu, X.; Ou, N. Simulating Flow of An Urban River Course with Complex cross Sections Based on the MIKE21 FM Model. *Water* **2020**, *12*, 761. [[CrossRef](#)]
31. Babu, M.T.; Kesava Das, V.; Vethamony, P. BOD–DO modeling and water quality analysis of a waste water outfall off Kochi, west coast of India. *Environ. Int.* **2006**, *32*, 165–173. [[CrossRef](#)] [[PubMed](#)]

Disclaimer/Publisher's Note: The statements, opinions and data contained in all publications are solely those of the individual author(s) and contributor(s) and not of MDPI and/or the editor(s). MDPI and/or the editor(s) disclaim responsibility for any injury to people or property resulting from any ideas, methods, instructions or products referred to in the content.